INFLUENCE OF LASER NOISE
ON THE OPTICALLY PUMPED,
ATOMIC-BEAM CLOCK

J. C. Camparo
Electronics and Photonics Laboratory
The Aerospace Corporation
PO Box 92957, Los Angeles, CA 90009, USA

Abstract

The optically pumped atomic-beam clock offers the potential for orders-of-magnitude improvement over conventional beam clocks. In part, this improvement stems from the use of diode lasers to efficiently prepare the atoms prior to entering the Ramsey cavity region and then to efficiently probe the atoms after they have passed through the cavity. However, while the diode lasers typically used in these beam clocks are single-mode devices, the quantum-noise associated with the single-mode is often non-negligible. Here, we describe our efforts to construct a realistic computer model of the clock, taking into account the multilevel nature of the atom along with the pump and probe lasers' amplitude and frequency fluctuations. Our goal is to develop a numerical means for generating the clock signal's time series, and in this way to isolate those laser-related processes that may play an important role in the clock's performance.

INTRODUCTION

Over the past several years, there has been considerable interest in employing single-mode diode lasers in various types of atomic clocks [1]. In the gas-cell frequency standard, efforts focus on replacing the lamp of the conventional clock with a diode laser. Not only does this replacement provide a greater signal-to-noise ratio [2], but additionally an ability to construct all-optical devices, thereby eliminating the microwave cavity from the gas-cell clock and the concomitant microwave power dependence of the clock's frequency [3]. In the case of the cesium-beam atomic clock, optical-pumping with diode lasers and optical detection of the clock signal improves the clock's signal-to-noise ratio and results in more symmetric microwave spectra [4]. Additionally, the use of diode lasers eliminates the conventional "A" and "B" magnets, thereby reducing the clock's weight and removing the potential for Majorana transitions.

Though single-mode diode lasers produce highly coherent fields, relative to the Rb and Cs atoms' energy level spacings, the phase noise of these lasers is not necessarily negligible. Since there is little mode partition noise in a single-mode diode laser (i.e., $\delta I/\langle I \rangle \sim 10^{-6}$ [5]), the principal source of noise in the laser is associated with a random walk of the laser field's phase, hence the reference to this type of field as a phase-diffusion-field or PDF [6]. (Note, however, that at low Fourier frequencies the laser's phase noise is dominated by flicker noise [7].) Typically, the laser's noise is parametrized by the laser linewidth, γ_L, which for conventional diode lasers is on the order of 50 MHz; for DBR diode lasers the linewidths are on the order of 2 MHz, and for external-cavity lasers the linewidths are ~ 0.1 MHz.

Given the important role that laser fluctuations play in the resonant field-atom interaction [8], we have initiated a project to study the influence of laser noise, both the laser's phase noise and its amplitude noise

(albeit relatively small), on the performance of the optically pumped atomic-beam clock. Laser noise influences the performance of the clock in two distinct ways, corresponding to the two roles of laser light in the clock's operation. In the optical-pumping region, laser noise can give rise to fluctuations in the ground state population distribution that enters the microwave cavity and, hence, the clock-signal amplitude. This noise will not only depend on the efficiency of generating a population imbalance between the atom's ground state hyperfine levels, but also on the population distribution *among* the Zeeman sublevels of a given hyperfine level. Thus, in order to understand fully optical-pumping noise, one needs to be cognizant of a potential role for the density matrix's higher order moments (e.g., the first moment or atomic polarization term, the second moment or atomic alignment term, etc.) [9]. In the fluorescence detection region, laser noise will again give rise to fluctuations in the clock signal. However, given the nonlinear relationship between laser frequency and fluorescence signal, there is the potential for various laser Fourier noise components to be mixed down into the clock signal's detection bandwidth.

Here, we describe the status of our investigations. Since our work focuses on determining the fluctuations in various clock parameters, and not simply their mean values, we do not solve the density matrix equations in steady state, but rather for the temporal evolution of the density matrix as the atom responds to the laser's fluctuating phase and amplitude. In the next section, we will describe our theoretical model and the simplifications we have employed in order to make the numerical calculations tractable. Then in the following section, we provide some of our recent results. We conclude with a discussion of future plans.

COMPUTATION

In the case of the real cesium atom (i.e., Cs^{133}), the $^2S_{1/2}$ ground state degeneracy is 16 (i.e., $F_g = 3,4$), while the $^2P_{3/2}$ excited state degeneracy for the two hyperfine levels under consideration in our work (i.e., $F_e = 4,5$) is 20. Thus, in the optical pumping region, where the $F_g=4$ and $F_e=4$ levels are coupled by the laser, we could potentially need to solve 624 simultaneous differential equations with time-dependent coefficients in order to model the system. Additionally, in the fluorescence detection region, where the $F_g=4$ and $F_e=5$ levels are coupled in order to take advantage of the cycling transition's large number of resonantly scattered photons per atom, we could potentially need to solve 399 simultaneous differential equations. Moreover, these 1,023 differential equations would have to be repeated for a number (e.g., 10) different velocity groups in order to model the beam's atomic speed distribution. Some simplification of this problem is obviously required in order to make it computationally manageable. We have therefore chosen to replace the real Cs^{133} isotope in our calculations (nuclear spin, I, equal to 7/2) with a fictitious Cs^{129} isotope (I = 1/2) having a stable lifetime, instead of a 32-hour half-life and a nuclear magnetic moment equal to that of Cs^{133}.

We confine our consideration to a situation in which the laser beams in both the optical-pumping region and the fluorescence detection region are linearly polarized with their polarization directions perpendicular to the atomic beam's quantization axis. Thus, the laser induces $\Delta m_F = \pm1$ transitions. Therefore, we only need to solve 18 and 31 simultaneous differential equations in the optical-pumping and fluorescence-detection regions, respectively, for our fictitious Cs^{129} isotope. As illustrated in Fig. 1, the laser induces excited and ground state coherences (shown as dashed lines in the figure) in both the optical-pumping and fluorescence-detection regions. In the optical-pumping region, these coherences correspond to two-photon transitions, while in the fluorescence-detection region we have coherences that correspond to two-, three-, and four-photon transitions. It is worth noting that in the case of the real Cs^{133} atom, we would have to account for coherences that are associated with *10-photon* transitions. Consequently, since as a general rule the order of the photon process determines the highest order of field-correlation function that can play a role in the stochastic-field/atom interaction, there is the potential for the clock's operation to depend on very high-order correlation functions of the diode laser's field. To include the effects of a magnetic field

on the Zeeman energy level spacing, we modify the magnetic moment of our Cs^{129} isotope so the $m_F = \pm F$ states shift in a magnetic field by an amount equal to that of the real Cs atom's $m_F = \pm F$ states.
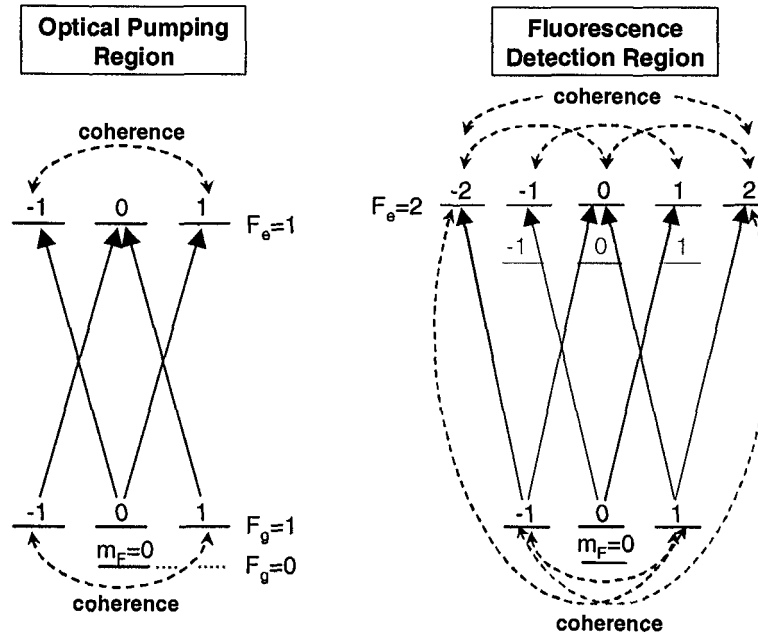

Figure 1: Illustration of the density matrix couplings that occur in the optical-pumping and fluorescence-detection regions. Solid lines correspond to laser one-photon transitions; dashed lines correspond to coherences that the laser/atom interaction creates. The energy levels correspond to our fictitious Cs^{129} isotope with nuclear spin 1/2.

We model our field as a single-mode diode laser (i.e., a phase-diffusion-field) with a linewidth of 100 kHz and a nearly lorentzian spectrum: γ_L is the full-width half-maximum of the field spectrum and β is a parameter that controls the fall-off of the lineshape's wings [8]. For the work here, β always equals $10^3 \gamma_L$. Additionally, to include the effects of laser-frequency-locking, we modulate the frequency of this field at 100 kHz, with a modulation index of 20 (i.e., $\Delta f_{mod} = \pm 2$ MHz). Unless otherwise noted, the parameters of Table I are employed in all of our simulations.

RESULTS IN THE OPTICAL-PUMPING REGION

Figure 2 shows the population in our fictitious isotope's $F_g = 0$ state and the rms value of the fluctuations in this population at the output of the optical-pumping region for a weak laser beam (i.e., $I_o = 0.12$ mW/cm²). The dashed line corresponds to the population in the $F_g = 0$ state in the absence of optical pumping. The double-peaked structure in the noise is consistent with expectations for a phase-diffusion field, in that the rms value of the noise should be proportional to the absolute value of the population curve's derivative (i.e., the curve of open diamonds). Note, however, that the noise does not go to zero on resonance, even though the derivative of the population curve would be zero there. We believe that this is due to the relative intensity noise on the diode laser that is included in our computations.

Table I: Parameters used in the numerical computations of a cesium beam interacting with a stochastic field.

Parameter	Value
Monovelocity Beam: v_{atom}	2.7×10^4 cm/sec
Field-Atom Interaction Length in Both Regions	0.4 cm
Static Magnetic Field	500 mG
γ_L	0.1 MHz
Laser RIN ($\delta I/\langle I \rangle$)	10^{-6}
Laser Intensity	12 mW/cm^2
Laser Frequency Modulation Rate	0.1 MHz
Laser Frequency Modulation Index	20

Figure 3 corresponds to the angular momentum orientation, $\langle F_z \rangle$, in the $F_g = 1$ level along with the rms value of the noise in $\langle F_z \rangle$ at the output of the optical-pumping region for a weak laser beam. $\langle F_z \rangle$ is defined as the population in the $|F_g=1,m_F=1\rangle$ state minus the population in the $|F_g=1,m_F=-1\rangle$ state. Though the average orientation is zero when the laser is tuned on resonance, the laser's frequency fluctuations give rise to noise in the atomic orientation. Preliminary calculations suggest that the laser's frequency modulation sets up a rotating angular momentum, which implies that the phenomenon may be associated with the $|F_g=1,m_F=-1\rangle \leftrightarrow |1,1\rangle$ coherence that the laser/atom interaction creates. Some evidence for this conclusion is presented in Figure 4, where $\langle F_z \rangle$ is shown as a function of field atom interaction time in the optical pumping region, which is controlled by v_{atom}.
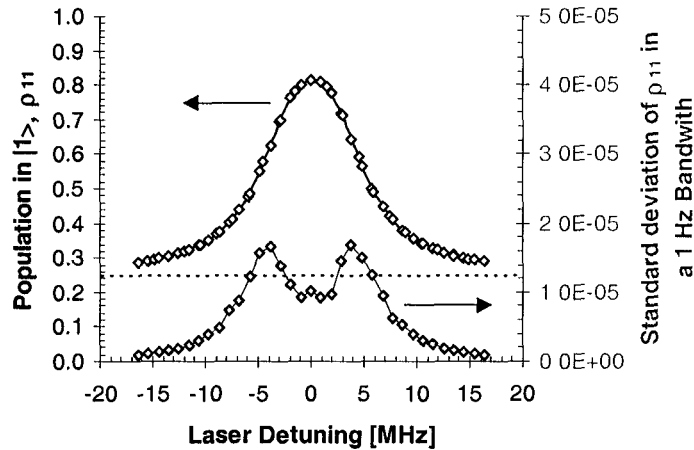

Figure 2: Population (open diamonds) and population noise (filled diamonds) in the $F_g = 0$ level as a function of laser tuning for low light intensity. In the absence of optical pumping, the $F_g = 0$ level population is 0.25.

Figure 5 is similar to Fig. 2 in that we present our results of the $F_g = 0$ population and its fluctuations as a function of laser detuning. In this case, however, we consider the nominal laser intensity of 12 mW/cm^2. The laser intensity is so strong that with the laser tuned near resonance optical pumping is easily completed prior to the atoms exiting the optical pumping region. Hence, laser frequency and amplitude fluctuations have little effect on the population in the $F_g = 0$ state.
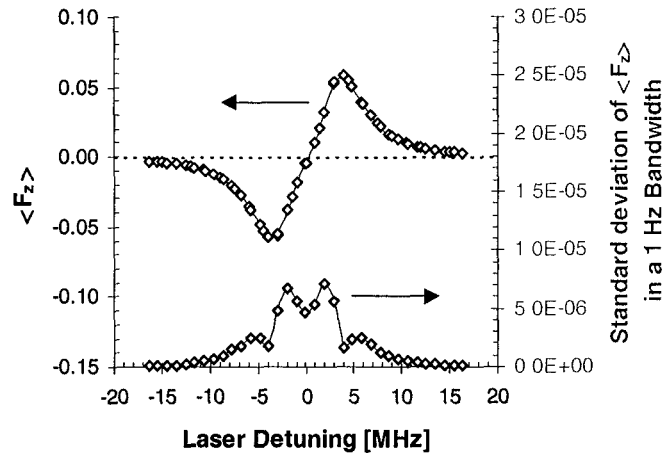

Figure 3: Angular momentum orientation, $\langle F_z \rangle$, (open diamonds) and orientation noise (filled diamonds) in the $F_g = 1$ level as a function of laser tuning for low light intensity. $\langle F_z \rangle$ is defined as the difference in population between the $m_F = 1$ and $m_F = -1$ states in the $F_g = 1$ ground state hyperfine level.
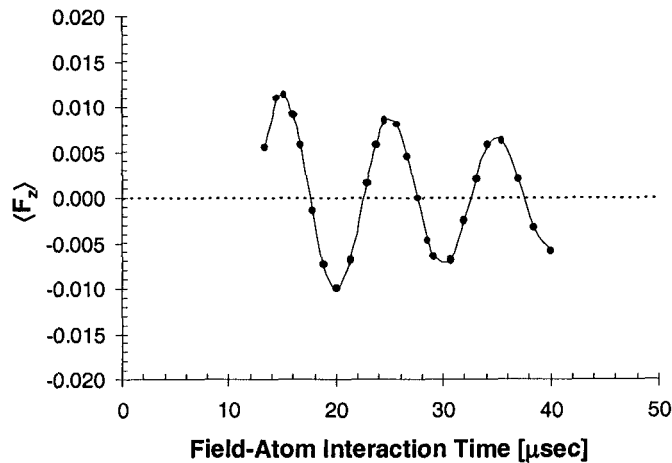

Figure 4: Angular momentum orientation, $\langle F_z \rangle$, as a function of field-atom interaction time. For these calculations, $\langle I \rangle = 12$ mW/cm^2 and B = 56 mG.
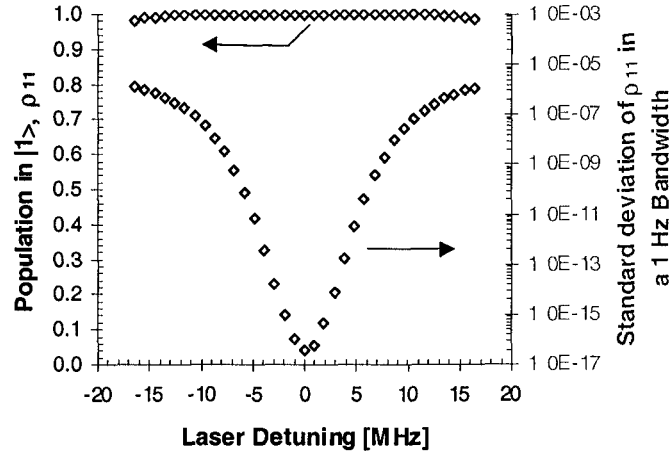
Figure 5: Population (open diamonds) and population noise (filled diamonds) in the $F_g = 0$ level as a function of laser tuning for high light intensity. For a broad range of laser detunings, all of the atomic population is in the $F_g = 0$ state.

Figure 6a shows the magnetic field dependence of the $F_g = 0$ state population and population noise. As indicated in Figure 1, the laser/atom interaction creates atomic coherences that oscillate at a frequency equal to the Zeeman splitting of the states involved in the coherence. At low magnetic fields, the Zeeman splitting is small and the coherences oscillate slowly. The consequence of this slow oscillation is that atomic population becomes "trapped" in the coherence and cannot be optically pumped into the $F_g = 0$ state. Therefore, even though the light intensity is high (i.e., 12 mW/cm^2), the optical pumping is not complete, and only ~ 70% of the population can be placed in the $F_g = 0$ hyperfine level. As the magnetic field increases, the coherences oscillate more rapidly, so that during the time the atoms are in the optical-pumping region the coherence oscillates many times and effectively averages to zero (i.e., the coherence "decouples" from the atomic evolution). With the loss of coherence, population is no longer trapped, and the optical-pumping process is able to proceed to completion. Notice that the noise has an extremum at approximately 80 mG, the same field strength that leads to decoupling, and that in the regime of low magnetic fields the rms population noise increases as B^2. We are presently studying the relationship between population noise and magnetic field in order to elucidate this quadratic dependence.

Figure 6b shows the dependence of $F_g = 0$ population and population noise on v_{atom}. As is intuitively obvious, since slow atoms spend a long time in the optical-pumping region, our results show that at low speeds optical pumping is complete with the consequence of little population noise. Notice that this is true for atoms with $v_{atom} \le 1000$ m/sec. Consequently, given the Maxwell speed distribution of atoms in a thermal beam, it seems unlikely that the beam's spread of velocities should have any significant effect on the efficiency of optical pumping or the rms noise in the $F_g = 0$ population.
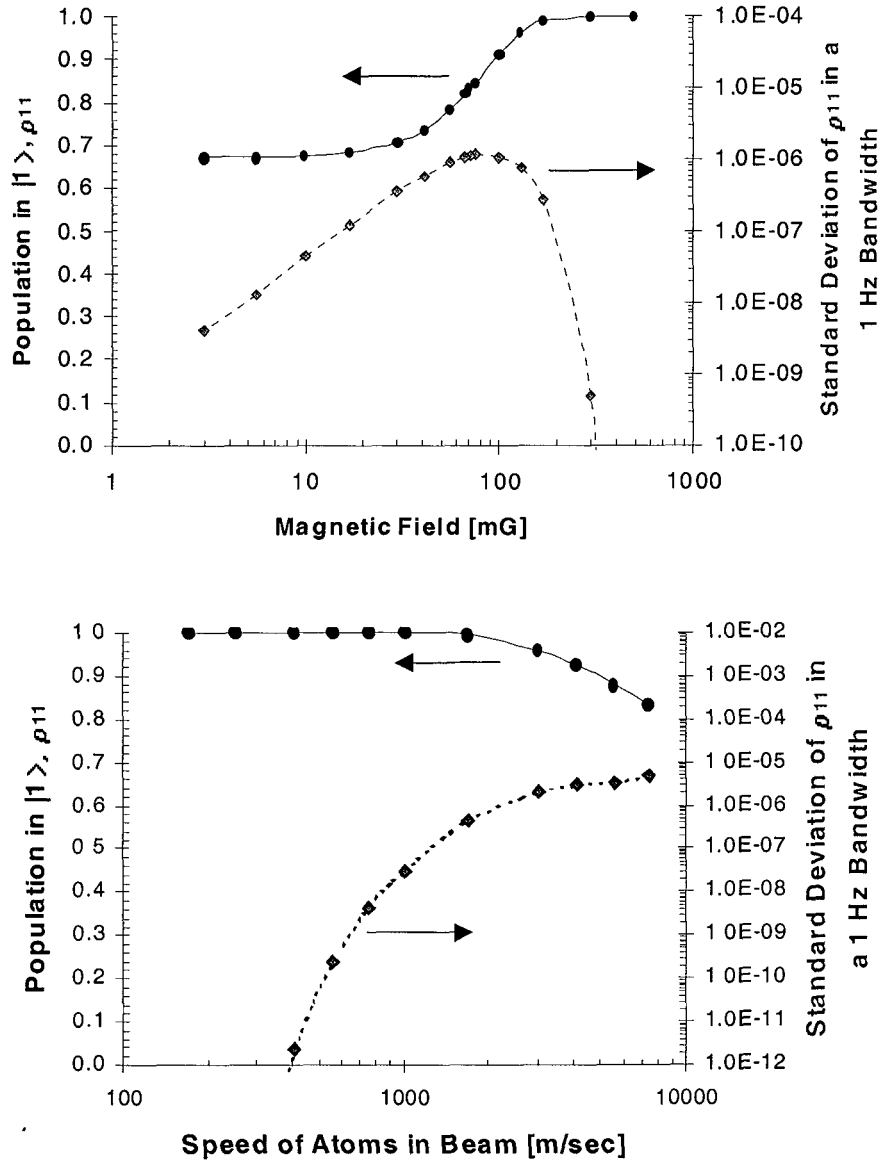
Figure 6: (a) Population and population noise in the $F_g = 0$ level as a function of static magnetic field strength in the optical-pumping region. (b) Population and population noise in the $F_g = 0$ level as a function of speed for the atoms in the beam.

FLUORESCENCE-DETECTION REGION

As is well known, the laser-induced-fluorescence (LIF) lineshape in the fluorescence-detection region will be a lorentzian of half-width half-maximum Δv_F:

$$\Delta v_F = \sqrt{\gamma_2^2 + \left(\frac{\gamma_2}{\gamma_1}\right)\omega_1^2} \ . \tag{1}$$

Here, γ_1 is the population relaxation rate, given by the Einstein-A coefficient, and γ_2 is the coherence

dephasing rate. ω_1 is the Rabi frequency, indicative of the strength of the field-atom interaction, and as is clear from Eq. (1) power-broadening of the fluorescence lineshape is amplified by the γ_2 to γ_1 ratio [10]. According to well-established theory [11], when LIF results from excitation with a phase-diffusion field the dephasing rate is increased by the PDF's linewidth:

$$\gamma_1 = A \qquad \text{and} \qquad \gamma_2 = \tfrac{1}{2}(A + \gamma_L).$$ (2)

Power broadening of the LIF lineshape is therefore amplified by a factor of $\tfrac{1}{2}\left(1 + \dfrac{\gamma_L}{A}\right)$.

Figure 7 shows our prediction of LIF in the fluorescence detection region for the case of a relatively weak, narrowband laser and zero static magnetic field: $I = 0.12$ mW/cm^2, $\gamma_L = 0.1$ MHz. For this laser intensity the Rabi frequency is 0.35 kHz. Circles correspond to the numerical results for the LIF signal, while diamonds correspond to the rms value of the fluorescence fluctuations. The solid curve is a lorentzian of full-width 5.16 MHz, the Cs $6^2P_{3/2}$ fluorescence decay rate. Note that the rms fluctuations have the functional form of the absolute value of the LIF signal's derivative.
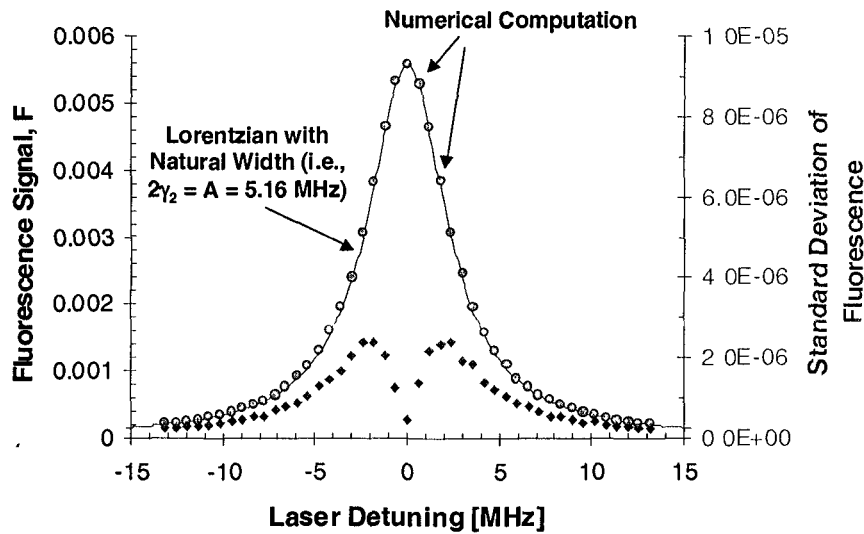

Figure 7: Laser-induced-fluorescence signal in the fluorescence detection region and the rms value of the fluorescence fluctuations. For these calculations, $I = 0.12$ mW/cm2, $\gamma_L = 0.1$ MHz and $B = 0$.

Figure 8 shows our prediction of the LIF signal when the field is broad. All parameters in the calculation are the same as in Figure 7, except that $\gamma_L = 10$ MHz. Again, circles correspond to the numerical results for the LIF signal, while diamonds correspond to the rms value of the fluorescence fluctuations. Note that the laser phase fluctuations have caused a broadening of the LIF lineshape. Given the values of A, γ_L and ω_1, the predicted lorentzian linewidth is 15.2 MHz, and is shown by the solid line passing through the data points. For comparison, we also show the LIF signal in the case of a monochromatic field. Note also that the fluorescence fluctuations have a maximum when the laser is tuned on-resonance. Though we are still

investigating this phenomenon, we belive that it may be due to "amplified" fluctuaions of the Rabi frequency associated with the laser's RIN. In the present case, the amplification factor for power broadening is $\gamma_2 / \gamma_1 = 1.47$.
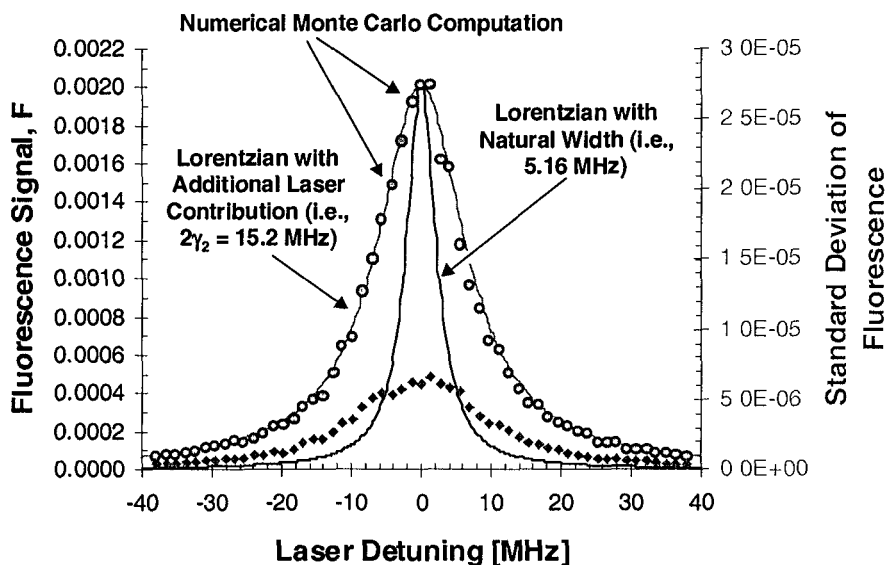

Figure 8: Laser-induced-fluorescence signal in the fluorescence detection region and the rms value of the fluorescence fluctuations. For these calculations, I = 0.12 mW/cm2, γ_L = 10 MHz and B = 0.

CONCLUSIONS

As discussed here, we have begun a theoretical project to study the role of laser phase and amplitude fluctuations in the operation of an optically pumped atomic beam clock. Regarding the optical-pumping region, we have found that in reasonably strong magnetic fields, on the order of 500 mG, ground state coherence terms do not trap atomic population. Consequently, with laser intensities in the range of tens of mW/cm^2 the optical-pumping process reaches completion and nearly all atoms are optically pumped into the non-absorbing hyperfine manifold. As a consequence, population fluctuations arising from the laser field are essentially nonexistent. Additionally, at these laser intensities the optical-pumping process is efficient for nearly all the atoms in a thermal atomic beam. Thus, we conclude that there is little effect of laser noise on the clock signal arising from the optical-pumping process.

With regard to the fluorescence detection region, the numerical simulation accurately captures the laser-phase fluctuations' contribution to the LIF signal. Though the atoms' speed distribution is not important for the optical-pumping region, it will likely be of significance in the fluorescence detection region, since slower moving atoms scatter more photons and, hence, contribute more to the total fluorescence signal. This will be especially important once the Ramsey cavity region is included in the computations. In future work, we plan to incorporate the beam's speed distribution into our simulations, and following this investigate the ability of the stochastic-field/atom interaction to down-convert high frequency laser noise into the clock signal's passband (i.e., the 10^2 to 10^3 Hz Fourier frequency range).

REFERENCES

[1] See for example: W. F. Buell, 1998, *"Laser-pumped and laser-cooled atomic clocks for space applications,"* **Laser and Particle Beams, 16**(4), 627.

[2] G. Mileti, J. Deng, F. L. Walls, D. A. Jennings, and R. E. Drullinger, 1998, *"Laser-pumped rubidium frequency standards: New analysis and progress,"* **IEEE Journal of Quantum Electronics, 34**(2), 233.

[3] J. Vanier, A. Godone, and F. Levi, 1998, *"Coherent population trapping in cesium: Dark lines and coherent microwave emission,"* **Physical Review, A58**(3), 2345.

[4] V. Giordano, A. Hamel, P. Petit, G. Theobald, N. Dimarcq, P. Cerez, and C. Audoin, 1991, *"New design for a high performance optically pumped cesium beam tube,"* **IEEE Transactions on Ultrasonics, Ferroelectrics, and Frequency Control, 38**(4), 350.

[5] J. Camparo, 1998, *"Conversion of laser phase noise to amplitude noise in an optically thick vapor,"* **Journal of the Optical Society of America, B15**(3), 1177.

[6] C. H. Henry, 1982, *"Theory of the linewidth of semiconductor lasers,"* **IEEE Journal of Quantum Electronics, 18**(2), 259.

[7] M. Ohtsu and S. Kotajima, 1984, *"Derivation of the spectral width of a 0.8 μm AlGaAs laser considering 1/f noise,"* Japanese Journal of Applied Physics, 23(6), 760; K. Kikuchi, 1989, *"Effect of 1/f-type FM noise on semiconductor laser linewidth residual in high-power limit,"* **IEEE Journal of Quantum Electronics, 25**(4), 684.

[8] See for example: J. Camparo and P. Lambropoulos, 1993, *"Monte Carlo simulations of field fluctuations in strongly driven resonant transitions,"* **Physical Review, A47**(1), 480.

[9] W. Baylis, 1978, *"Collisional depolarization in the excited state,"* in Progress in Atomic Spectroscopy: Part B, ed. W. Hanle and W. Kleinpoppen (Plenum Press, New York), pp. 1227-1297.

[10] N. Bhaskar, J. Camparo, W. Happer, and A. Sharma, 1981, *"Light narrowing of magnetic resonance lines in dense, optically pumped alkali-metal vapor,"* **Physical Review, A23**(6), 3048; J. Camparo and R. Frueholz, 1985, *"Linewidths of the 0-0 hyperfine transition in optically pumped alkali-metal vapors,"* **Physical Review, A31**(3), 1440.

[11] A. Georges and P. Lambropoulos, 1978, *"AC Stark splitting in doubly resonant three-photon ionization with nonmonochromatic fields,"* **Physical Review, A18**(2), 587.